



## RESEARCH LETTER

10.1002/2015GL065690

## Key Points:

- Strong shear flow spontaneously develops in the outflow region
- The shear flow is unstable to the electron Kelvin-Helmholtz instability
- K-H vortices continuously drive secondary reconnection and lead to the formation of islands

## Correspondence to:

Q. Lu,  
qmlu@ustc.edu.cn

## Citation:

Huang, C., Q. Lu, F. Guo, M. Wu, A. Du, and S. Wang (2015), Magnetic islands formed due to the Kelvin-Helmholtz instability in the outflow region of collisionless magnetic reconnection, *Geophys. Res. Lett.*, *42*, 7282–7286, doi:10.1002/2015GL065690.

Received 5 AUG 2015

Accepted 5 SEP 2015

Accepted article online 10 SEP 2015

Published online 29 SEP 2015

## Magnetic islands formed due to the Kelvin-Helmholtz instability in the outflow region of collisionless magnetic reconnection

Can Huang<sup>1,2</sup>, Quanming Lu<sup>1,2</sup>, Fan Guo<sup>3</sup>, Mingyu Wu<sup>1</sup>, Aimin Du<sup>4</sup>, and Shui Wang<sup>1</sup>

<sup>1</sup>CAS Key Laboratory of Geospace Environment, Department of Geophysics and Planetary Science, University of Science and Technology of China, Hefei, China, <sup>2</sup>Collaborative Innovation Center of Astronautical Science and Technology, Beijing, China, <sup>3</sup>Theoretical Division, Los Alamos National Laboratory, Los Alamos, New Mexico, USA, <sup>4</sup>Key Laboratory of Ionospheric Environment, Institute of Geology and Geophysics, Chinese Academy of Sciences, Beijing, China

**Abstract** We carry out large-scale particle-in-cell kinetic simulations to demonstrate that a super-Alfvénic electron shear flow across the current layer can be spontaneously generated in the outflow region of magnetic reconnection, which is unstable to the electron Kelvin-Helmholtz (K-H) instability. The resulted K-H vortex structures continuously drive the secondary magnetic reconnection and formation of secondary magnetic islands, which leads to strong electron energization in the outflow region.

### 1. Introduction

Magnetic reconnection suddenly releases magnetic free energy by rearranging magnetic field. It is widely discussed in solar [Giovannelli, 1946; Masuda *et al.*, 1994], planetary [Øieroset *et al.*, 2001; Wang *et al.*, 2010; Zhang *et al.*, 2012], and laboratory plasmas [Ji *et al.*, 1998; Li *et al.*, 2007; Dong *et al.*, 2012] and often invoked to explain plasma heating and acceleration [Vasyliunas, 1975; Biskamp, 2000; Priest and Forbes, 2000]. Previous kinetic studies primarily focused on the dynamics close to X lines, and the formation of secondary islands has been identified in the electron diffusion region [Drake *et al.*, 2006a; Daughton, 2006; Wang *et al.*, 2010]. These secondary islands (flux ropes in three-dimensional simulations) are considered to be generated by the tearing instability [Daughton *et al.*, 2011] or through the Kelvin-Helmholtz (K-H) instability driven by an external velocity shear [Fermo *et al.*, 2012]. They not only dramatically enhance the reconnection rate [Daughton, 2006] but are also beneficial to electron acceleration through Fermi process or coalescence of magnetic islands [Drake *et al.*, 2006b; Wang *et al.*, 2010; Oka *et al.*, 2010; Guo *et al.*, 2014].

Until now the outflow structure of magnetic reconnection and its related plasma energization are much less known. Observations at Earth's magnetotail have shown magnetic fluctuations in the outflow region of magnetic reconnection [Volwerk *et al.*, 2007]. The observations of solar flares indicate continuous particle energization as plasma flows in the plasma sheet [Fletcher and Hudson, 2008; Liu *et al.*, 2013], and the magnetic fluctuations in the outflow region have been suggested to be important for electron acceleration [Larosa and Moore, 1993]. However, to understand the plasma dynamics in the reconnection outflow region, a self-consistent kinetic simulation is desired.

In this work, by performing large-scale two-dimensional (2-D) particle-in-cell (PIC) simulations of magnetic reconnection with a finite guide field, we demonstrate that strong electron shear flow spontaneously develops in the outflow region. We find that the shear flow is unstable to the electron Kelvin-Helmholtz instability, and it results in multiple K-H vortices that continuously drive secondary reconnection and lead to the formation of magnetic islands. This process leads to strong electron energization in the outflow region, which may be important for a number of explosive phenomena such as solar flares and storms in planetary magnetospheres.

### 2. Simulation Model

The simulations start from a Harris current sheet equilibrium with a particle number density  $n(z) = n_b + n_0 \operatorname{sech}^2(z/\delta)$ , where  $n_b = 0.1n_0$  represents the background density and  $\delta = 0.5c/\omega_{pi}$  is the half width of the current sheet. The corresponding magnetic field is given by  $\mathbf{B}(z) = B_0 \tanh(z/\delta) \mathbf{e}_x + B_{y0} \mathbf{e}_y$ , where  $B_0$  is the asymptotical magnetic field and  $B_{y0} = B_0$  is the guide field. Both ions and electrons are assumed to have

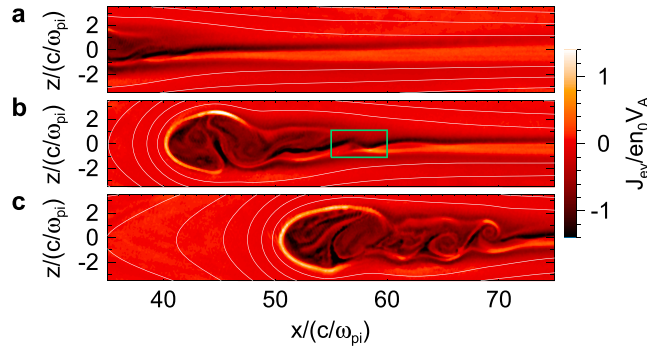


**Figure 1.** The time evolution of the electron out-of-plane current density at (a)  $\Omega_i t = 55$ , (b)  $\Omega_i t = 65$ , and (c)  $\Omega_i t = 75$  in the outflow region of the reconnection. The white lines represent the in-plane magnetic field lines.

is performed in the  $(x, z)$  plane, and a large-scale computational domain  $[-L_x/2, L_x/2] \times [-L_z/2, L_z/2]$  with  $L_x = 204.8c/\omega_{pi}$  and  $L_z = 25.6c/\omega_{pi}$  is used here. The spatial resolution is  $\Delta x = \Delta z = 0.05c/\omega_{pi}$ . The time step is set to be  $\Delta t = 0.001\Omega_i^{-1}$ , where  $\Omega_i = eB_0/m_i$  is the ion gyrofrequency. More than  $10^9$  particles for each species are employed in the simulation. Periodic boundary conditions are assumed in the  $x$  direction, while in the  $z$  direction conducting boundary conditions are retained and particles are specularly reflected at the boundaries.

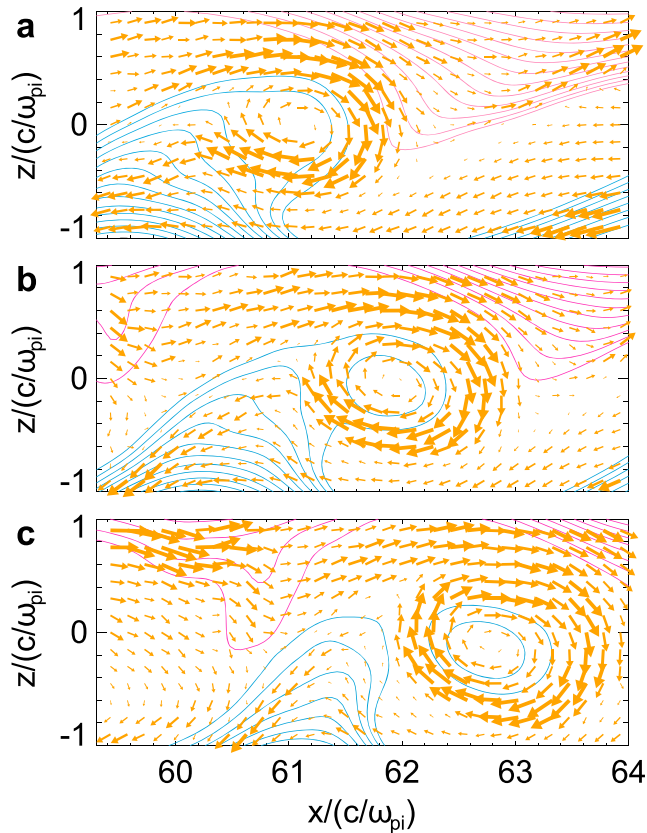


**Figure 2.** The enlarged view of the in-plane magnetic field lines and electron flow vectors in the outflow region at (a)  $\Omega_i t = 70$ , (b)  $\Omega_i t = 71$ , and (c)  $\Omega_i t = 72$ . It gives an image of the generation of the magnetic island in a Kelvin-Helmholtz vortex. The red and blue lines present the in-plane magnetic lines in the upper and lower half plane of the initial Harris current sheet. The arrows show the electron flow in the frame of the mean electron outflow  $\mathbf{V}_e + 0.8V_{Ai}\mathbf{e}_x$ .

Maxwellian velocity distributions, with an initial temperature ratio  $T_{i0}/T_{e0} = 5$  and a mass ratio  $m_i/m_e = 25$ , where the subscripts  $i$  and  $e$  stand for ion and electron, respectively. The light speed is assumed to be  $c = 15V_{Ai}$ , where  $V_{Ai}$  is the ion Alfvén speed based on  $B_0$  and  $n_0$ . The electromagnetic fields are defined on the grids and updated by integrating the Maxwell equations with an explicit leapfrog scheme, while the ions and electrons are treated as individual superparticles and advanced in these electromagnetic fields. The simulation

The reconnection is initiated by a small local flux perturbation centered at  $x = 0$ , and the perturbation has the form  $\Delta\psi = \psi_0 e^{-(x^2+z^2)/\delta^2} \cos(2\pi x/L_x) \cos(\pi z/L_z)$ . Here the initial disturbance amplitude  $\psi_0$  is set to  $0.05cB_0/\omega_{pi}$ .

### 3. Simulation Results

In our simulations, only one single X line, which appears around  $\Omega_i t = 15$ , develops in the middle of the current sheet (at  $x \approx 0$ ). The simulation domain is sufficiently large, which allows us to study the evolution of the exhaust region before the computational boundary can influence it. In Figure 1, we plot the time evolution of the out-of-plane electron current density  $J_{ey}$  in the outflow region, and magnetic field lines are also shown in the figure for reference. Around  $\Omega_i t = 65$ , the vortex structures of the out-of-plane electron current develop in the outflow region. As the time goes on, the vortex structures of the electron current become fully developed and propagate toward the downstream region with a sub-Alfvén speed of about  $0.8 V_{Ai}$ .

Figure 2 shows an enlarged view of the magnetic field lines and electron flow vectors in the outflow region at

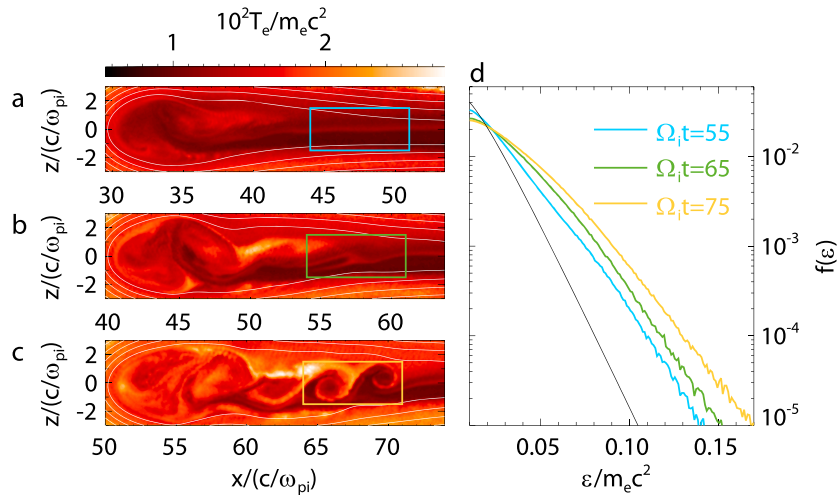


**Figure 3.** The snapshots of the electron temperature at (a)  $\Omega_i t = 55$ , (b)  $\Omega_i t = 65$ , and (c)  $\Omega_i t = 75$  in the reconnection outflow. The initial electron temperature in the plasma sheet is about  $0.01 m_e c^2$ , and the black curve shows the initial Maxwellian distribution. The white lines represent the in-plane magnetic field lines. (d) The electron energy spectra in the selected region marked with blue, green, and orange boxes are represented in the corresponding colors.

$\Omega_i t = 70, 71$ , and  $72$ , respectively. The magnetic field lines are twisted in the outflow region caused by the vortex structures of the out-of-plane electron currents, which leads to the generation of a thin current layer. Then, magnetic reconnection occurs around  $\Omega_i t = 70$ . During the reconnection, a magnetic island with the size of about one ion inertial length is formed and detached from the lower part of the current sheet. The magnetic island then propagates toward the downstream region with a speed about  $0.8 V_{A_i}$ . Similar processes for the generation of magnetic islands in a shear layer have also been discussed in the previous researches [Fermo *et al.*, 2012; Nykyri and Otto, 2001; Nakamura *et al.*, 2008; Nakamura and Fujimoto, 2008]. Here the process takes place spontaneously in the outflow of a magnetic reconnection region. In order to distinguish the reconnection in the outflow region from the primary reconnection at  $x \approx 0$ , we call the reconnection, which occurs later in the outflow region of the primary magnetic reconnection, as secondary reconnection, and the resulted islands as secondary islands. Electrons flow along the magnetic field lines at a high speed around the magnetic island, which forms a vortex. Note that in Figure 2, we only show the formation of one secondary island. Actually, in the whole outflow region of the primary reconnection, there are multiple secondary islands that continuously form due to the evolution of vortex structures.

With the proceeding of the secondary magnetic reconnection and the formation of secondary magnetic islands in the outflow region, we also find that the electrons in the outflow region can be strongly heated. Figure 3 shows the time evolution of the electron temperature in the outflow region and the electron energy spectrum in the selected region. Around  $\Omega_i t = 65$ , the vortex structures and secondary magnetic islands begin to develop in the outflow region. From the figure, we can find that accompanied with the generation of the vortex structures and magnetic islands, the electrons are highly heated with the temperature about 2–3 times of that just before the formation of secondary magnetic islands (around  $\Omega_i t = 55$ ). However, we can also find that there is still another process of electron heating before  $\Omega_i t = 65$ . Such a heating process has been previously studied in Wu and Shay [2012] and Huang *et al.* [2014], which is caused when the electrons are reflected by the enhanced magnetic field which is piled up by the plasma jet from the reconnection site, and simultaneously, the electron shear flow is formed in the outflow region.

To identify the generation mechanism of these vortex structures and the secondary magnetic reconnection in the outflow region of the primary reconnection, we show the distributions of the electron bulk velocity in such a vortex structure at  $\Omega_i t = 65$ , when the structures begin to develop. Figure 4a plots the distribution of the electron bulk velocity in the  $x$  direction  $V_{ex}$  while Figure 4b shows the profiles of the drift velocity  $-E_z/B_y$ , electron bulk velocity along the  $x$  direction  $V_{ex}$  and the half local electron Alfvén speed  $|V_{A_{ex}}|/2$  along the  $z$  direction. A shear flow of electron velocity can be obviously found in the outflow region. In the lower part of the current sheet, the electron bulk velocity is  $V_{ex} \approx -0.2V_{A_i}$  while in the upper part the electron bulk

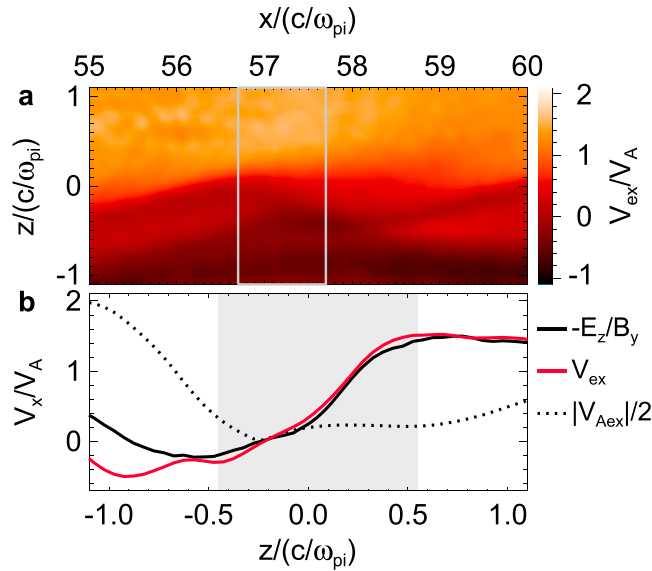


**Figure 4.** A zoom in of the region within the green box in Figure 1b. (a) The electron bulk velocity in the x direction and (b) the profiles of drift velocity  $-E_z/B_y$ , electron bulk velocity  $V_{ex}^x$  and the local electron Alfvén speed  $|V_{Aex}|/2$  along the z direction. The value is averaged within  $57.7c/\omega_{pi} \leq x \leq 58.7c/\omega_{pi}$  which is denoted with the gray box in Figure 4a.

velocity is  $V_{ex} \approx 1.6V_{Ai}$ . The velocity shear can be seen more clearly in Figure 4b. Note that the electron bulk velocity is consistent with the drift velocity, which means that in this region electrons are frozen and roll up the magnetic field lines. This velocity shear may be unstable to K-H instability; however, it must also overcome any stabilizing effects from the magnetic field in the direction of streaming associated with Alfvén waves or whistler waves. For the electron K-H instability to develop within an electron current sheet, the characteristic growth rate must exceed the whistler frequency. The instability criterion is  $\Delta V_{ex} > |V_{Aex}|/2$  [Fermo et al., 2012], where  $V_{Aex}$  is the x component of the local electron Alfvén speed. As demonstrated in the shadow region in Figure 4b, where the shear flow exists, the dotted line shows  $|V_{Aex}|/2 \leq 0.4V_{Ai}$  while  $\Delta V_{ex} \approx 1.8|V_{Aex}|$ .

It is consistent with the criterion of the electron K-H instability. Note that ions are decoupled from the magnetic field lines while the motions of electrons change the topology of the magnetic field during the formation of the magnetic island. At the same time, the half width of the shear flow can be estimated to be about  $0.4 c/\omega_{pi}$ , and according to the theory [Gaur and Das, 2012], the wavelength of the fastest-growing mode of the electron K-H instability is about  $5.0 c/\omega_{pi}$ . From Figure 3c, the average length of these vortex structures is about  $4.2 c/\omega_{pi}$ , and our simulation result is roughly consistent with the predicted value from the theory.

#### 4. Conclusions and Discussion

In summary, by performing a large-scale PIC simulation of magnetic reconnection in a current sheet with a guide field, we investigate the formation of the turbulent current sheet and the resulted secondary reconnection in the outflow region of the primary magnetic reconnection. After the primary magnetic reconnection occurs in the center of the simulation domain, a strong electron shear flow develops in the outflow region, and the current sheet in the outflow region is unstable to the electron K-H instability, which leads to the formation of the twisted current sheet with vortex structures. In such a twisted current sheet, secondary reconnection continuously occurs and leads to the formation of magnetic islands; at last electrons are strongly energized. The formation of secondary magnetic island has been previously reported in the vicinity of the X line due to the tearing instability [Daughton, 2006] or electron K-H instability driven by an electron shear flow [Fermo et al., 2012], which can greatly enhance the reconnection rate. In this work, we find that secondary magnetic reconnection can occur and then magnetic islands are generated in the outflow region of magnetic reconnection. Electrons can also be significantly energized in the current sheet.

Although a strong guide field ( $B_{y0} = B_0$ ) is used in this letter, our simulations have shown that such kind of secondary islands may also be generated in the outflow region when the guide field is as weak as  $0.3 B_0$ . Such an amplitude of the guide field may exist in either the magnetotail or magnetopause reconnection. Therefore, the secondary islands generated in the outflow region of the primary reconnection due to the excitation of the electron K-H instability can be expected to be observed by satellite observations in both the magnetotail and magnetopause reconnection. Actually, secondary islands have been observed in the outflow region of the magnetotail reconnection [Eastwood et al., 2007], and the electron K-H instability may provide a generation mechanism for such kind of secondary islands.

### Acknowledgments

This research was supported by the National Science Foundation of China, grants 41331067, 41204103, 11220101002, 11235009, and 41274144, 973 Program (2013CBA01503 and 2012CB825602), Ph.D. Programs Foundation of Ministry of Education of China (20123402120010), and the Specialized Research Fund for State Key Laboratories, CAS Key Research Program KZZD-EW-01-4. The results are generated from our computer simulation code. The data can be obtained by contacting the corresponding author through e-mail (qmlu@ustc.edu.cn).

The Editor thanks two anonymous reviewers for their assistance in evaluating this paper.

### References

- Biskamp, D. (2000), *Magnetic Reconnection in Plasmas*, 3 pp., Cambridge Univ. Press, Cambridge, U. K.
- Daughton, W., J. Scudder, and H. Karimabadi (2006), Fully kinetic simulations of undriven magnetic reconnection with open boundary conditions, *Phys. Plasmas*, *13*, 072101.
- Daughton, W., V. Roytershteyn, H. Karimabadi, L. Yin, B. J. Albright, B. Bergen, and K. J. Bowers (2011), Role of electron physics in the development of turbulent magnetic reconnection in collisionless plasmas, *Nat. Phys.*, *7*, 539–542.
- Dong, Q. L., et al. (2012), Plasmoid ejection and secondary current sheet generation from magnetic reconnection in laser-plasma interaction, *Phys. Rev. Lett.*, *108*, 215001.
- Drake, J. F., M. Swisdak, K. M. Schoeffler, B. N. Rogers, and S. Kobayashi (2006a), Formation of secondary islands during magnetic reconnection, *Geophys. Res. Lett.*, *33*, L13105, doi:10.1029/2006GL025957.
- Drake, J. F., M. Swisdak, H. Che, and M. A. Shay (2006b), Electron acceleration from contracting magnetic islands during reconnection, *Nature*, *443*, 553–556.
- Eastwood, J. P., T.-D. Phan, F. S. Mozer, M. A. Shay, M. Fujimoto, A. Retinò, M. Hesse, A. Balogh, E. A. Lucek, and I. Dandouras (2007), Multi-point observations of the Hall electromagnetic field and secondary island formation during magnetic reconnection, *J. Geophys. Res.*, *112*, A06235, doi:10.1029/2006JA012158.
- Fermo, R. L., J. F. Drake, and M. Swisdak (2012), Secondary magnetic islands generated by the Kelvin-Helmholtz instability in a reconnecting current sheet, *Phys. Rev. Lett.*, *108*, 255005.
- Fletcher, L., and H. S. Hudson (2008), Impulsive phase flare energy transport by large-scale Alfvén waves and the electron acceleration problem, *Astrophys. J.*, *675*, 1645.
- Gaur, G., and A. Das (2012), Linear and nonlinear studies of velocity shear driven three dimensional electron-magnetohydrodynamics instability, *Phys. Plasmas*, *19*, 072103.
- Giovanelli, R. G. (1946), A theory of chromospheric flares, *Nature*, *158*, 81.
- Guo, F., et al. (2014), Formation of hard power laws in the energetic particle spectra resulting from relativistic magnetic reconnection, *Phys. Rev. Lett.*, *113*, 155005.
- Huang, C., Q. Lu, S. Lu, P. Wang, and S. Wang (2014), The effect of a guide field on the structures of magnetic islands formed during multiple X line reconnections: Two-dimensional particle-in-cell simulations, *J. Geophys. Res. Space Physics*, *119*, 798–807, doi:10.1002/2013JA019249.
- Ji, H. T., M. Yamada, S. Hsu, and R. Kulsrud (1998), Experimental test of the Sweet-Parker model of magnetic reconnection, *Phys. Rev. Lett.*, *80*, 3256–3259, doi:10.1103/PhysRevLett.80.3256.
- Larosa, T. N., and R. L. Moore (1993), A mechanism for bulk energization in the impulsive phase of solar flares: MHD turbulent cascade, *Astrophys. J.*, *418*, 912.
- Li, C. K., F. H. Séguin, J. A. Frenje, J. R. Rygg, R. D. Petrasso, R. P. Town, O. L. Landen, J. P. Knauer, and V. A. Smalyuk (2007), Observation of Megagauss-field topology changes due to magnetic reconnection in laser-produced plasmas, *Phys. Rev. Lett.*, *99*, 055001, doi:10.1103/PhysRevLett.99.055001.
- Liu, W., Q. Chen, and V. Petrosian (2013), Plasmoid ejections and loop contractions in an eruptive M7.7 solar flare: Evidence of particle acceleration and heating in magnetic reconnection outflows, *Astrophys. J.*, *767*, 168.
- Masuda, S., T. Kosugi, H. Hara, S. Tsuneta, and Y. Ogawara (1994), A loop top hard X-ray in a compact solar flare as evidence for magnetic reconnection, *Nature*, *371*, 495–497, doi:10.1038/371495a0.
- Nakamura, T. K. M., and M. Fujimoto (2008), Magnetic effects on the coalescence of Kelvin-Helmholtz vortices, *Phys. Rev. Lett.*, *101*, 165002.
- Nakamura, T. K. M., M. Fujimoto, and A. Otto (2008), Structure of an MHD-scale Kelvin-Helmholtz vortex: Two-dimensional two-fluid simulations including finite electron inertial effects, *J. Geophys. Res.*, *113*, A09204, doi:10.1029/2007JA012803.
- Nykyri, K., and A. Otto (2001), Plasma transport at the magnetospheric boundary due to reconnection in Kelvin-Helmholtz vortices, *Geophys. Res. Lett.*, *28*, 3565–3568, doi:10.1029/2001GL013239.
- Øieroset, M., T. D. Phan, M. Fujimoto, R. P. Lin, and R. P. Lepping (2001), In situ detection of collisionless reconnection in the Earth's magnetotail, *Nature*, *412*, 414–417, doi:10.1038/35086520.
- Oka, M., M. Fujimoto, I. Shinohara, and T. D. Phan (2010), "Island surfing" mechanism of electron acceleration during magnetic reconnection, *J. Geophys. Res.*, *115*, A08223, doi:10.1029/2010JA015392.
- Priest, E., and T. Forbes (2000), *Magnetic Reconnection: MHD Theory and Applications*, 6 pp., Cambridge Univ. Press, Cambridge, U. K.
- Vasyliunas, V. M. (1975), Theoretical models of magnetic field line merging, *Rev. Geophys.*, *13*, 303–336, doi:10.1029/RG013i001p0303.
- Volwerk, M., K.-H. Glassmeier, R. Nakamura, T. Takada, W. Baumjohann, B. Klecker, H. Rème, T. L. Zhang, E. Lucek, and C. M. Carr (2007), Flow burst-induced Kelvin-Helmholtz waves in the terrestrial magnetotail, *Geophys. Res. Lett.*, *34*, L10102, doi:10.1029/2007GL029459.
- Wang, R. S., Q. M. Lu, A. M. Du, and S. Wang (2010), In situ observations of a secondary magnetic island in ion diffusion region and associated energetic electrons, *Phys. Rev. Lett.*, *104*, 175003, doi:10.1103/PhysRevLett.104.175003.
- Wu, P., and M. A. Shay (2012), Magnetotail dipolarization front and associated ion reflection: Particle-in-cell simulations, *Geophys. Res. Lett.*, *39*, L08107, doi:10.1029/2012GL051486.
- Zhang, T. L., et al. (2012), Magnetic reconnection in the near Venusian magnetotail, *Science*, *336*, 567–570, doi:10.1126/science.1217013.